

Department of Physics, Chemistry and Biology

Master's Thesis

Search for Dark Matter in the Upgraded High Luminosity LHC at CERN

Impact of ATLAS phase II performance on a mono-jet analysis

Sven-Patrik Hallsjö

Thesis work performed at Stockholm University

Linköping, June 4, 2014

LITH-IFM-A-EX--14/2863--SE



**Linköpings universitet
TEKNISKA HÖGSKOLAN**

Department of Physics, Chemistry and Biology
Linköping University
SE-581 83 Linköping, Sweden

Search for Dark Matter in the Upgraded High Luminosity LHC at CERN

Impact of ATLAS phase II performance on a mono-jet analysis

Sven-Patrik Hallsjö

Thesis work performed at Stockholm University

Linköping, June 4, 2014

Supervisor: **Docent Christophe Clément**
 FYSIKUM Stockholm University
Professor Magnus Johansson
 IFM, Linköping University

Examiner: **Professor Magnus Johansson**
 IFM, Linköping University



Avdelning, Institution
Division, Department

Theoretical physics group
Department of Physics, Chemistry and Biology
SE-581 83 Linköping

Datum
Date

2014-06-04

Språk
Language

Svenska/Swedish
 Engelska/English

Rapporttyp
Report category

Licentiatavhandling
 Examensarbete
 C-uppsats
 D-uppsats
 Övrig rapport

ISBN
—

ISRN
LITH-IFM-A-EX--14/2863--SE

Serietitel och serienummer **ISSN**
Title of series, numbering —

URL för elektronisk version

<http://urn.kb.se/resolve?urn=urn:nbn:se:liu:diva-XXXXX>

Titel Sökandet efter mörk materia i den uppgraderade hög luminositets LHC i CERN
Title Search for Dark Matter in the Upgraded High Luminosity LHC at CERN

Undertitel Påverkan av ATLAS fas II prestanda på en mono-jet analys
Subtitle Impact of ATLAS phase II performance on a mono-jet analysis

Författare Sven-Patrik Hallsjö
Author

Sammanfattning
Abstract

Something as an introduction:

The LHC at CERN is undergoing an upgrade to increase the center of mass energy for the colliding particles which means that new physical processes will be explored. One drawback of this is that it will be harder to isolate unique particle collisions since more and more collisions will occur simultaneously, so called pile-up.

One hope for the upgrade is that WIMP models of dark matter will be detected.

This thesis covers looking at effective operators which try to explain dark matter without adding new theories to the standard model or QFT.

Some results and a slight conclusion.

Nyckelord

Keywords ATLAS, Beyond standard model physics, CERN, Dark matter, Elementary particle physics, High energy physics, something, this is in mythesis.sty

4 Abstract

5 Something as an introduction:

6 The LHC at CERN is undergoing an upgrade to increase the center of mass en-
7 ergy for the colliding particles which means that new physical processes will be
8 explored. One drawback of this is that it will be harder to isolate unique parti-
9 cle collisions since more and more collisions will occur simultaneously, so called
10 pile-up.

11 One hope for the upgrade is that WIMP models of dark matter will be detected.

12 This thesis covers looking at effective operators which try to explain dark matter
13 without adding new theories to the standard model or QFT.

14 Some results and a slight conclusion.

15 **Acknowledgments**

16 I wish to dedicate this thesis to my mathematics teacher Ulf Rydmark without
17 whom I would not have studied physics.

18 A big thank you to my family, fiancée and friends who have supported me through-
19 out my education. A warm thank you to my friend Joakim Skoog who altered
20 some of the images for me.

21 I want to thank my supervisor Christophe Clément and all those who helped me
22 at Stockholm University.

23 I also want to thank my examiner Magnus Johansson, who always took time to
24 answer any question from and support his students.

25 A special thank you to Professor Irina Yakimenko without whom my master years
26 would have been duller and probably impossible.

27 Finally I want to thank someone someone for proofreading my

Linköping, June 2014
Sven-Patrik Hallsjö

Contents

Notation**1 Introduction**

1.1	Research goals	2
1.2	Theoretical Background	3
1.2.1	Quantum mechanics and quantum field theory	3
1.2.2	Nuclear, particle and subatomic particle physics	4
1.2.3	The standard model of particle physics	4
1.2.4	Dark matter	5
1.2.5	Effective field theory	6
1.2.6	Search for WIMPS	8
1.3	Experimental overview	10
1.3.1	LHC	10
1.3.2	ATLAS	11
1.3.3	Coordinate system	12
1.3.4	Reconstructing data	12
1.3.5	Pile-up	13
1.3.6	Mono-jet analysis	13
1.3.7	Phase II high luminosity upgrade	14
1.3.8	Monte Carlo simulation	15

2 Validation of smearing functions

2.1	Smearing functions	18
2.1.1	Electron and photon	18
2.1.2	Muon	18
2.1.3	Tau	18
2.1.4	Jets	18
2.1.5	Missing Transversal Energy	18
2.2	Validation	20
2.3	Results	21
2.3.1	Electron and photon	22
2.3.2	Muon	23
2.3.3	Tau	23

63	2.3.4 Jets	24
64	2.3.5 Missing Transversal Energy	25
65	2.4 Expected results	26
66	2.5 Discussion	28
67	2.5.1 Smearing independent on pile-up	28
68	2.5.2 Comparison to expected results	28
69	2.6 Conclusion	29
70	3 Evaluating dark matter signals	31
71	3.1 Signal to background ratio	31
72	3.1.1 Selection criteria	32
73	3.1.2 Verifying background data	32
74	3.1.3 Figures of merit	33
75	3.1.4 D5 operators	34
76	3.1.5 Light vector mediator models	34
77	3.1.6 Susy models?	34
78	3.2 Other selection criteria and observables	34
79	3.3 Mitigating the effect of the high luminosity	34
80	3.4 Results	35
81	3.4.1 Limit on M^*	35
82	3.4.2 Effect of pile-up on M^*	35
83	3.4.3 Previous results	36
84	3.4.4 Limit on mediator mass	36
85	3.4.5 Effect of pile-up on mediator mass	36
86	3.5 Discussion	36
87	3.6 Conclusion	36
88	4 Results and Conclusions	37
89	4.1 Validation of smearing functions	37
90	4.2 Signal to background ratio	37
91	4.2.1 Limit on M^*	37
92	4.2.2 Limit on mediator mass	37
93	4.3 Other selection criteria and observables	37
94	4.3.1 Limit on M^*	37
95	4.3.2 Limit on mediator mass	37
96	4.4 Mitigating the effect of the high luminosity	37
97	4.5 Recommendations to mitigate the effect of the high luminosity	37
98	4.6 Suggestions for future research	38
99	A Datasets	41
100	A.1 Background processes	41
101	A.1.1 Validation	41
102	A.1.2 Background to signals	41
103	A.2 D5 signal processes	42
104	A.3 Light vector mediator processes	42
105	Bibliography	47

Notation

NOTATIONS

Notation	Explanation
barn(b)	$1 \text{ barn}(b) = 10^{-24} \text{ cm}^2$
\oplus	$a \oplus b = \sqrt{a^2 + b^2}$, $a \oplus b \oplus c = \sqrt{a^2 + b^2 + c^2}$

ABBREVIATIONS

Abbreviation	Expansion
ATLAS	A large Toroidal LHC ApparatuS
CERN	Organisation européenne pour la recherche nucléaire ¹
CMS	Compact Muon Solenoid
LHC	Large Hadron Collider
RMS	Root Mean Square
SM	the Standard Model of particle physics
WIMP	Weakly Interacting Massive Particle
WIMPS	Weakly Interacting Massive ParticleS
QED	Quantum ElectroDynamics
QFT	Quantum Field Theory
QM	Quantum Mechanics

¹Originally, Conseil Européen pour la Recherche Nucléaire

1

Introduction

112 Discrepancies in measurements of the rotations of galaxies indicate the presence
113 of a large amount of matter which interacts through gravity, though not elec-
114 tromagnetically making it invisible to our telescopes. This matter is commonly
115 referred to as dark matter. Since no known or hypothesised particle in the stan-
116 dard model of particle physics can be used as a candidate for dark matter, this
117 hints at the presence of new physics.

118 At the Organisation Européene pour la Recherche Nucléaire (CERN) focus now
119 lies to discover any evidence of so called weakly interacting massive particles
120 (WIMPS) which may be a candidate for dark matter. It is usually impossible to
121 detect any interaction of dark matter candidates on the subatomic scale, however
122 through looking at proposed interactions, searching for assumed decay channels
123 and by investigating what is invisible to the detectors by using momentum con-
124 servation it is hoped that signs will be found. Though to date, none have been
125 found.

126 Both experiments and current theories now show that higher energies are re-
127 quired at the LHC to be able to see any signs. This is why the LHC and all detectors
128 are undergoing a vast upgrade program [1]. In this thesis focus will be on the last
129 part of the upgrade due for completion in 2023, known as the high luminosity-
130 LHC phase II upgrade; and also on the ATLAS detector. The method used in this
131 thesis focuses on looking at data which emulate conditions at the upgraded LHC.

132 1.1 Research goals

133 This research took place at Stockholm University from January 7th until **when**?

134 During the research period the following tasks were set up and performed/answered:

- 135 • Implement a C++ programme that loops over the collisions inside the signal
136 and background datasets.
- 137 • For each collision retrieve the relevant observables (variables used to extract
138 the signal over the background) and apply "smearing functions" to emulate
139 the effect of the high luminosity on the observables.
- 140 • For both signal and background datasets, compare observables before and
141 after smearing. What observables are the least/most affected?
- 142 • Implement selection criteria that selects the signal collisions efficiently while
143 reduces significantly the background. In a first step the selection criteria
144 should be taken from existing studies.
- 145 • Selection criteria can be evaluated and compared with each other using a
146 figure of merit P , that measures the sensitivity of the experiment to the dark
147 matter signal. Calculate P for the given selection criteria before and after
148 smearing.
- 149 • What is the effect of the high luminosity (smearing) on the value of P ?
- 150 • Investigate other selection criteria and observables, to mitigate the effect of
151 high luminosity. Use P to rank different criteria after smearing.
- 152 • Conclude on the effect of the high luminosity on the sensitivity for dark matter
153 and possible ways to mitigate its effects using alternative observables
154 and selection criteria.

1.2 Theoretical Background

1.2.1 Quantum mechanics and quantum field theory

In the beginning of the 20th century, some physical phenomena could not be explained by classical physics, for example the ultra-violet disaster of any classical model of black-body radiation, and the photoelectric effect [2]. It was these phenomena that led to the formulation of quantum mechanics (QM), where energy transfer is quantized and particles can act as both waves and particles at the same time [3].

Combining QM with classical electromagnetism proved harder than expected, colliding a photon(em-field) and an electron (particle/wave) is quite tricky. This can be seen when trying to calculate the scattering between them both in a QM schema. One idea that came from this was to explain them both in the same framework, field theory. Also, trying to incorporate special relativity into QM suggested a field description where space-time is described using the metric formalism from differential geometry. The culmination of both of these problems is the first part of a Quantum field theory (QFT), Quantum electrodynamics (QED) which with incredible precision explains electromagnetic phenomena including effects from special relativity[4]. It is in this merging that antimatter was theorised, since it is a requirement for the theory to hold. After the discovery of antimatter, the theory was set in stone. Since this the theory has been altered somewhat to explain more and more experimental data. This is discussed more in subsection 1.2.2 and subsection 1.2.3.

To be able to calculate properties in QFT one uses the Lagrangian formalism [5], which gives a governing equation for the different physical processes. In general the Lagrangian used for the Standard model is quite complicated, one can thus focus on one of the different terms corresponding to a specific interaction. This can be done to calculate the so called cross-section for a process, which is related to the probability that that process will occur. A step to simplify the calculations is to use the so called Feynman diagrams, an example of which is given in figure 1.1.

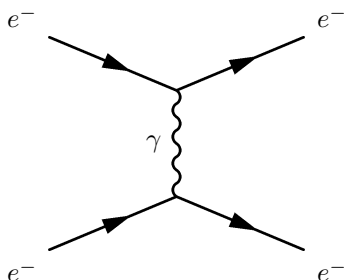


Figure 1.1: An example of a Feynman diagram explaining an electron-electron scattering using QED.

Through the figure, which comes with certain rules, and knowing what the major process (in this case QED) one can calculate the cross-section [4]. It is this that is needed to predict what one will be able to detect new particles.

188 1.2.2 Nuclear, particle and subatomic particle physics

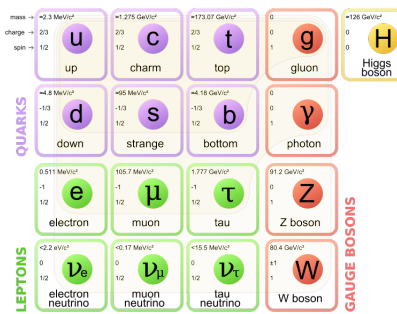
189 Many could argue that these branches of physics started after Ernest Rutherford
 190 famous gold foil experiment [6], where he discovered that matter is composed of
 191 matter with a nucleus, a lot of empty space and electrons.

192 It was this that sparked the curiosity to see what the nucleus is made of and
 193 what forces govern the insides of atoms. After this, and the combination of the
 194 theoretical description given by QM, a lot more has been discovered and still
 195 more has been predicted. The newest of these is of course the Higgs particle,
 196 which was predicted through QFT and then discovered by the ATLAS and the CMS
 197 experiments at CERN [7].

198 The discovered particles are often divided into different groups depending on
 199 the fundamental particles that build them up. For instance, particles build up of
 200 three quarks are known as hadrons. Particles with an integer spin are known as
 201 bosons whereas half-integer particles are known as fermions.

202 1.2.3 The standard model of particle physics

203 The standard model of particle physics, referred to simply as the standard model
 204 (SM), is the particle zoo which tries to categorize all the particles and that have
 205 been discovered experimentally. QFT explains the interactions between these par-
 206 ticles and it has also predicted several particles by including symmetries [6]. Re-
 207 garding SM, Gauge bosons are the force carriers for the different forces, quarks
 208 are the and leptons are the fundamental blocks that we know of so far. The differ-
 ence between the later two is if they interact via the strong force or not.



209 **Figure 1.2:** The standard model of
 210 particle physics where the three first
 211 columns represent the so called genera-
 212 tions, starting with the first. [8].

213 SM is today the pinnacle of particle physics and can be used to explain almost
 214 everything that occurs around us. There are however some problems [9]:

- 215 • There is no link between gravity and the SM.
- 216 • Asymmetry between matter and antimatter can not be fully explained.
- 217 • No dark matter candidate!
- 218 • No explanation that can contain dark matter.

216 In this thesis focus lies with dark matter, some more introduction to possible
 217 dark matter and different candidates in extensions to SM are explained in subsection
 218 1.2.4.

219 1.2.4 Dark matter

220 Dark matter is among other things, the name given to the solution to the discrepancies
 221 of galactic rotations.

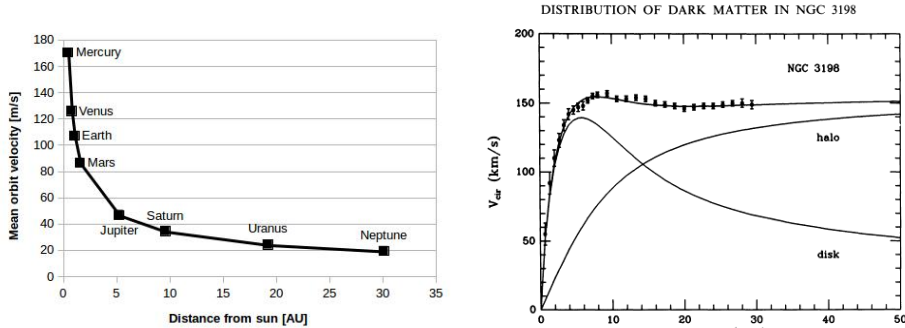
222 To explain this, focus on matter in a galaxy which are rotating around the center
 223 of the galaxy. Through Newtons law of gravity and the centrifugal force one can
 224 calculate the rotation speed dependent on the distance to the center of the galaxy.
 225 Since one of these forces is attractive and the other repulsive, if the matter is in
 226 a stable orbit around the galactic center (which they are) they must be equal and
 227 give us an expression for the speed depending on the distance. Newtons law can
 228 be written as the following:

$$F_{Gravitational} = G \frac{Mm}{r^2} = G_M \frac{m}{r^2} \quad F_{Centrifugal} = m \frac{V^2}{r} \quad (1.1)$$

229 where G is the gravitational constant, M the mass of the centre object, m the mass
 230 of the matter, r the distance between the two and V is the rotation speed. It has
 231 been simplified using G_M since all matter orbits the same galactic center. Setting
 232 the equations in (1.1) results in:

$$G_M \frac{m}{r^2} = m \frac{V^2}{r} \Leftrightarrow V^2 = \frac{G_M}{r} \Rightarrow V = \sqrt{\frac{G_M}{r}} \propto \frac{1}{\sqrt{r}} \quad (1.2)$$

233 where the speed is assumed to be positive and \propto means proportional. Through
 234 these simple calculations it shown that the rotation speed should decrease with
 235 and increased distance. The same reasoning can be applied to our solar system
 236 where this is the case figure 1.3a. The relation in these units is $V = \frac{107}{\sqrt{r}}$ where
 237 107 can be used in (1.2) to calculate the mass of the sun. However when looking
 238 at galaxies, even when taking into account that one has to see the galaxies as a
 239 mass distribution and that the above is only true when outside of the inner mass
 240 half, this is not the case! In figure 1.3b experimental data can be seen from the
 241 galaxy NGC3198 with a fitted curve which does not decrease with the distance
 242 but is instead constant. This is the discrepancy which is solved by postulating
 243 the existence of dark matter. After this the big question arises, what could this
 244 dark matter consist of? What is known so far lies in the name. It is called dark
 245 since there is no electromagnetic interaction and matter since it has gravitational
 246 interaction. This means that it can not be made up of any baryonic matter or
 247 anything in the Standard Model apart from neutrinos. The main interest of this
 248 thesis and also the main contributor to the rotational discrepancies is known as
 249 cold dark matter. This is due to the matter having a low speed, thus low kinetic
 250 energy, and have a high particle mass (In the GeV scale) [9, 12, 13]. This means
 251 however that neutrinos can not be a candidate, thus dark matter can not be made
 252 out of any standard model particles. There are several ideas to detected dark
 253 matter, [9]



(a) *Rotation speed of planets in our solar system. Since the distance is quite small on an astronomical scale, there is no sign of dark matter. Based on data from [10].*

(b) *Rotation speed of matter in NGC3198 with a curve fitting and three different models, if only a dark model halo existed, if there was no dark matter and the correct, if both exist [11].*

Figure 1.3: Different rotation curves, both for planets in our solar system and matter in the NGC3198 galaxy.

- Ordinary matter interacting with ordinary matter can produce dark matter, known as production. Which is the processes that occurs at particle accelerators.
- Dark matter interacting with ordinary matter can produce dark matter, known as direct detection.
- Dark matter interacting with dark matter can produce ordinary matter, known as indirect detection.

In this thesis the focus lies with production. There are several theories how to detect dark matter in proton-proton collisions such that occur at the LHC at CERN this is covered more in subsection 1.2.6.

1.2.5 Effective field theory

In quantum field theory the objective is usually to find the part of the Lagrangian which explains a type of interaction, known as the operator of the interaction and also to find the probability amplitude (cross-section) for a certain interaction. For complicated processes it is easier to employ certain conditions so that the small scale phenomena are simplified and the whole picture understood. This is known as using an effective field theory and the concept is explained in figure 1.4. The operator can be found through assuming the possible interactions and using the effective field theory [4]. The cross-sections can be found through the Feynman diagrams as described in subsection 1.2.1.

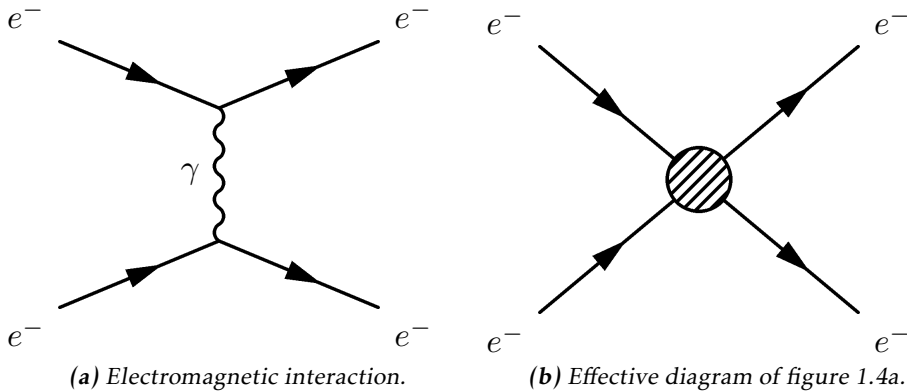


Figure 1.4: Feynman diagram of an electron-electron scattering, both as an ordinary diagram and as its effective theory version, where the details are hidden in the blob.

In this thesis the same effective field theory as in Refs. [12, 14] will be considered. The WIMP (usually denoted χ) is assumed to be the only particle in addition to the standard model fields. It is assumed that an even number of χ must be in every coupling. It is assumed that the mediator exists is heavier than the WIMPS, meaning that their interactions are in higher order terms of the effective field theory and thus not included in the operators. For simplicity, the WIMPS are assumed to be SM singlets, thus invariant under SM gauge transformations, and the coupling to the Higgs boson is neglected.

The operators used in this thesis are assumed to be quark bilinear operators on the form $\bar{q}\Gamma q$ where Γ is a 4×4 matrix of the complete set,

$$\Gamma = \{1, \gamma^5, \gamma^\mu, \gamma^\mu \gamma^5, \sigma^{\mu\nu}\} \quad (1.3)$$

This will dictate how the operators are written, more of why this is done can be found in [4, 12, 14].

This defines an effective field theory of the interaction of singlet WIMPs with hadronic matter. It is an approximation which will break down when the mediator mass is close to the mass of the WIMP. The condition for this is derived in [14] and gives:

$$M > 2m_\chi \quad (1.4)$$

where m_χ is the mass of the WIMP and M is the mass of the mediator particle. There is also the requirement that:

$$M \lesssim 4\pi M_* \quad (1.5)$$

where M_* is the energy scale where the effective theory is no longer a good approximation.

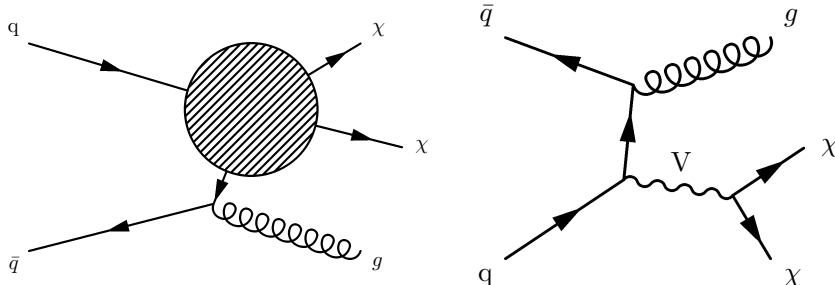
²⁹⁴ In this work, WIMPS are assumed to be Dirac fermions (half integer spin and is
²⁹⁵ not its own antiparticle).

²⁹⁶ In table 1.1 the operators which are integrated out via the effective field theory
²⁹⁷ and are of interest in this thesis are given.

Name	Initial state	Type	Operator
D1	qq	scalar	$\frac{m_q}{M_*^3} \bar{\chi} \chi \bar{q} q$
D5	qq	vector	$\frac{1}{M_*^2} \bar{\chi} \gamma^\mu \chi \bar{q} \gamma_\mu q$
D8	qq	axial-vector	$\frac{1}{M_*^2} \bar{\chi} \gamma^\mu \gamma^5 \chi \bar{q} \gamma_\mu \gamma^5 q$
D9	qq	tensor	$\frac{1}{M_*^2} \bar{\chi} \sigma^{\mu\nu} \chi \bar{q} \sigma_{\mu\nu} q$
D11	gg	scalar	$\frac{1}{4M_*^3} \bar{\chi} \chi \alpha_s (G_{\mu\nu}^a)^2$

Table 1.1: Table based on discussion in [13].

²⁹⁸ Where D denotes that the WIMPS are assumed to be Dirac fermions. These can all
²⁹⁹ be described using figure 1.5a.



(a) Effective Feynman diagram explaining the D-operators. **(b)** Feynman diagram describing the vector mediator model.

Figure 1.5: Feynman diagrams describing the signal models used in this thesis.

³⁰⁰ Another model which is considered is a vector mediator model which is described
³⁰¹ by figure 1.5b.

302 1.2.6 Search for WIMPS

³⁰³ The search for WIMPS is based on a mono-jet analysis which is described in sub-
³⁰⁴ section 1.3.6. This method revolves around a high energetic jet which arises from
³⁰⁵ the gluon from figure 1.5b and momentum missing from the energy conservation.

306 This means that something has happened which the detectors can not detect. If
307 the models from subsection 1.2.5 can explain the missing energy, then a model
308 for WIMPS has been found.

309 Since the search for WIMPS at the LHC is based on looking at the missing energy,
310 not actual detection, the experiment can not establish if a WIMP is stable on a
311 cosmological time scale and thus if it is a dark matter candidate [13]. This means
312 that if a candidate is found, it may still not be the dark matter that is needed to
313 explain the cosmological observations.

314 The different theories discussed in subsection 1.2.5 require some process in which
315 quarks and anti-quarks are produced. At ATLAS they have looked at proton-
316 proton collisions, in which they are produced, with 8 TeV center of mass energy
317 with out finding any excess of mono-jet events. This is why it is very interesting
318 that the LHC is undergoing a upgrade that will allow higher energy levels, see
319 subsection 1.3.7. With this the processes can be given higher energy and thus the
320 produced particles can be comprised of higher mass.

321 1.3 Experimental overview

322 1.3.1 LHC

323 The large hadron collider (LHC) is a particle accelerator located at CERN near
 324 Geneva in Switzerland, see figure 1.6. The accelerator was built to explore physics
 325 beyond the standard model and to make more accurate measurements of stan-
 326 dard model physics. Before it was shut down for an upgrade in 2012 it was able
 327 to accelerate two proton beams to such a velocity that each proton in them had
 328 an energy of 4 TeV which gives a center of mass energy, $\sqrt{s} = 8$ TeV. The proton
 329 beam is comprised of bunches of protons with enough spacing that bunch col-
 330 lisions can happen independent of each other. Apart from the energy, the rate at
 331 which the accelerator produces a certain process can be calculated through the
 332 instantaneous luminosity. For the LHC the instantaneous luminosity was 10^{34}
 333 $\text{cm}^{-2}\text{s}^{-1}$ [15] or $10\text{nb}^{-1}\text{s}^{-1}$ where 1 barn(b) = 10^{-24} cm^2 .

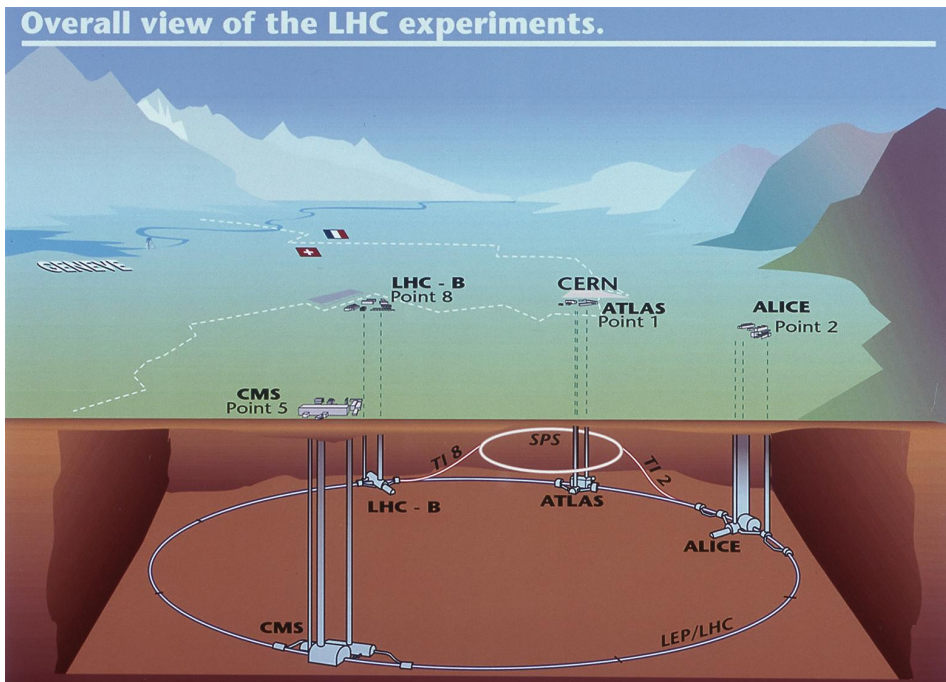


Figure 1.6: Figure showing the LHC and the different detector sites[16].

334 The instantaneous luminosity, often just denoted luminosity, can be defined in
 335 different ways depending on how the collision takes place. For two collinear
 336 intersecting particle beams it is defined as:

$$\mathcal{L} = \frac{f k N_1 N_2}{4\pi \sigma_x \sigma_y} \quad (1.6)$$

337 where N_i are the number of protons in each of the bunches, f is the frequency
 338 at which the bunches collide , k the number of colliding bunches in each beam,
 339 and σ_x (σ_y) is the horizontal (vertical) beam size at the interaction point. Since
 340 the instantaneous luminosity increases quadratically with more protons in each
 341 bunch, increasing the number of protons would be a good strategy to increase
 342 the instantaneous luminosity. However aside from the difficulties to create and
 343 maintain a beam with more particles, a large N_i increases the probability for
 344 multiple collisions per bunch crossing, referred to as pile-up. Pile up will be a
 345 key aspect which is described more in subsection 1.3.5.

346 The expected number of events can be calculated by using the instantaneous lu-
 347 minosity through the following:

$$N = \sigma \int \mathcal{L} dt \equiv \sigma \mathcal{L} \quad (1.7)$$

348 where \mathcal{L} is the integrated luminosity and σ is the cross section which is often
 349 measured in barn. The integrated luminosity is a measurement of total number
 350 of interactions that have occurred over time. Before the LHC was shut down \mathcal{L}
 351 was 20.8 fb^{-1} .

352 The cross section, as explained in subsection 1.2.1, is a measure of the effective
 353 surface area seen by the impinging particles, and as such is expressed in units
 354 of area. The cross section is proportional to the probability that an interaction
 355 will occur. It also provides a measure of the strength of the interaction between
 356 the scattered particle and the scattering center. Further details can be found in
 357 reference [17].

358 1.3.2 ATLAS

359 As seen in figure 1.6, there are several detectors at the LHC. One of these is
 360 ATLAS which is a general purpose detector that uses a toroid magnet. Its goal
 361 is to observe several different production and decay channels. The detector is
 362 composed of three concentric sub-detectors, the Inner detector, the Calorimeters
 363 and the Muon spectrometer [18].

364 The Inner detectors main task is to detect the tracks of the particles. It also mea-
 365 sures the position of the initial proton-proton collision.

366 The Calorimeters, electromagnetic and hadronic, are used to calculate the energy
 367 contained in the different particles. The electromagnetic detects particles which
 368 are charged, and the hadronic those which are neutral.

369 The Muon spectrometer is used to detect signs of muons, which will simply pass
 370 through the other detectors without leaving a trace. It also calculates the energy
 371 and momentum of the muons.

372 The neutrinos escape the ATLAS experiment without being detected, and in this
 373 thesis it is assumed that WIMPS pass through all the detectors without leaving
 374 any trace.

375 1.3.3 Coordinate system

376 The coordinate system of ATLAS, seen in figure 1.7 is a right-handed coordinate
 377 system with the x-axis pointing towards the centre of the LHC ring, and the z-axis
 378 along the tunnel/beam (counter clockwise) seen from above. The y-axis points up-
 379 ward. The origin is defined as the geometric center of the detector. A cylindrical
 380 coordinate system is also used for the transversal plane, (R, ϕ, Z) . For simplicity
 381 the pseudorapidity of particles from the primary vertex is defined as:

$$\eta = -\ln(\tan \frac{\theta}{2}) \quad (1.8)$$

382 where θ is the polar angle (xz-plane) of the particle direction measured from
 383 the positive z-axis. η is through this definition invariant under boosts in the z-
 384 direction.

385 It is quite common to calculate the distance between particles and jets in the
 386 (η, ϕ) space, $d = \sqrt{(\Delta\eta)^2 - (\Delta\phi)^2}$.

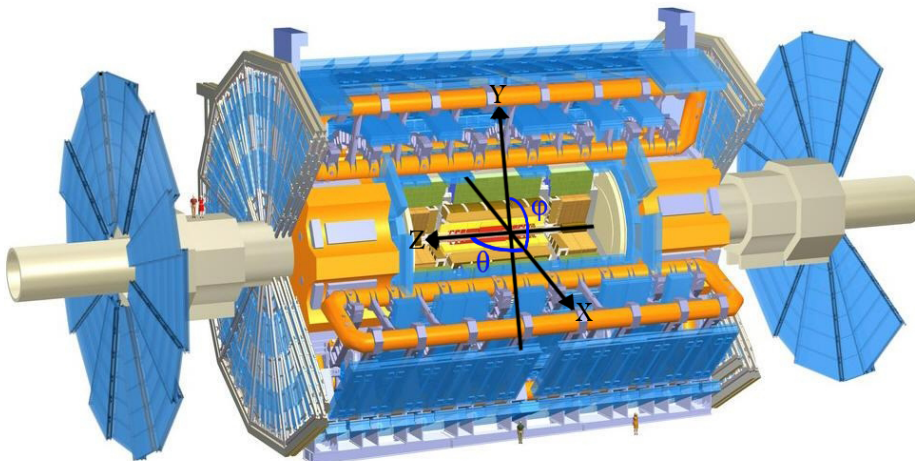


Figure 1.7: The ATLAS detector and the definition of the orthogonal Cartesian coordinate system. Image altered from[19]

387 1.3.4 Reconstructing data

388 To be able to compare the simulated data to real data it is important to include
 389 effects of the detectors. This is done using so called smearing functions which try
 390 to emulate the reconstruction of data.

391 The reconstruction process of data [18] is based on what response is given from
 392 the detectors. It is affected by pile-up and the energy of that which is detected.
 393 This process is not specifically used in the thesis, however the smearing functions
 394 are discussed in section 2.1.

395 1.3.5 Pile-up

396 Pile-up is the phenomena that several proton-proton collisions occur simultaneously.
 397 The number of pile-up is defined as the average number of proton-proton
 398 collisions that occur per bunch crossing per second. It is denoted as $\langle \mu \rangle$. μ can
 399 be calculated by adjusting a Poisson distribution to fit the curve created by the
 400 number of interactions per bunch crossing at a given luminosity. When this is
 401 done μ will be the mean value of the Poisson distribution.

402 1.3.6 Mono-jet analysis

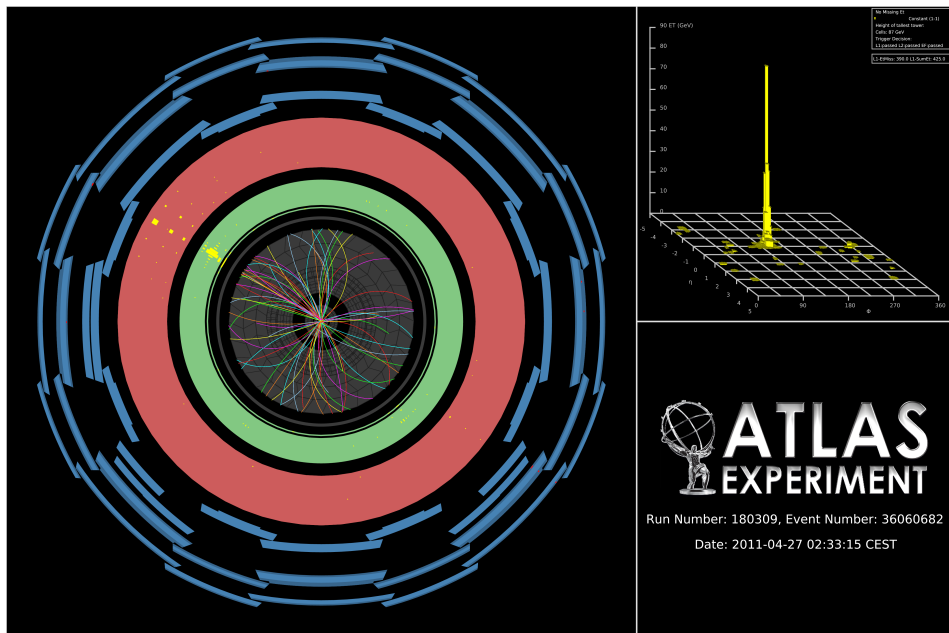


Figure 1.8: Image of an actual mono-jet event recorded by the ATLAS experiment [20].

403 When measuring the transversal energy one can in some interactions find incon-
 404 sistencies, such as jets that are in excess in one direction. In figure 1.8 one can see
 405 a high energetic jet which gives an excess of transversal energy in one direction
 406 after the collision. Since there is no balancing jet there must be transverse energy
 407 that is not detected, denoted E_T^{Miss} , since it was close to zero before the collision.
 408 This gives an indication that there energy to balance this that simply can not be
 409 detected. This could for instance be neutrinos or the sign of a new particle.

410 E_T^{Miss} is the modulus of the E_T^{Miss} vector which is defined as:

$$E_T^{\vec{M}iss} = -\sum E_T^{\vec{jet}} - \sum E_T^{\vec{Electron}} - \sum E_T^{\vec{\mu}on} - \sum E_T^{\vec{T}au} - \sum E_T^{\vec{\gamma}on} \quad (1.9)$$

411 Jets are hadrons which travel in the same direction and are usually created from

hadronization of a quark or a gluon in a collision. Usually jets are composed of a lot of energetic hadrons.

Since the jets are created from quarks or gluons, measuring a jet results in more information about the collision.

There are two main classes of events, signal and background. The signal corresponds to events that would arise from one of the processes in subsection 1.2.5. However to know that the missing energy is sign of the signal then one must understand all the other components that could contribute to the missing energy. Also there must be an excess of missing energy from what is expected from the background.

The background comprises of standard model processes that can mimic the mono-jet signature.

1.3.7 Phase II high luminosity upgrade

At the moment, the whole LHC is undergoing a step by step upgrade program which will be finalized around 2022-2023, denoted the high luminosity upgrade, or HL-upgrade. The upgrade consists of different stages, meaning that the upgrade will halt for periods so that experiments can take place. In figure 1.9 one can see

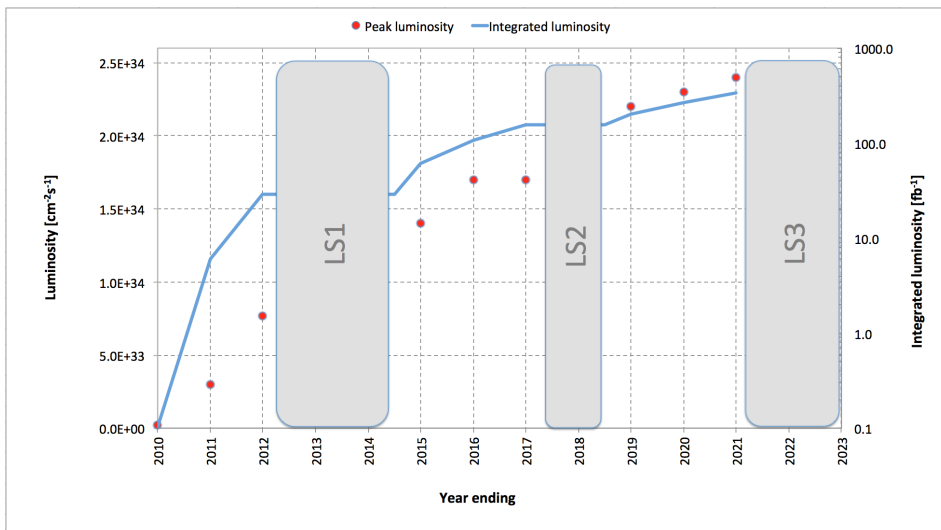


Figure 1.9: A graph showing the upgrading timetable with the instantaneous luminosity, denoted luminosity, and integrated luminosity expected in the different stages.

the three proposed upgrades. The period before LS1 is denoted phase 0, after LS1 and before LS2 phase I and after LS3 phase II.

LS1 is the upgrade which will take the LHC to its designed performance.

- 432 LS2 will take the LHC to the ultimate designed instantaneous luminosity.
 433 LS3 which is the focus of this thesis, will increase the instantaneous luminosity
 434 even more. Though for this to happen a modification of the whole LHC
 435 must be done, instead of just an upgrade and maintenance as before.

- 436 The following is expected for the experiments done after phase II:

Entity	Expected	Last run (2012)
Instantaneous luminosity	$\mathcal{L} \sim 50 \text{ nb}^{-1} \text{s}^{-1}$	$\mathcal{L} \sim 10 \text{ nb}^{-1} \text{s}^{-1}$
Integrated luminosity	$\mathcal{L} = 1000 - 3000 \text{ fb}^{-1}$	$\mathcal{L} = 20 \text{ fb}^{-1}$
Pile-up	$\langle \mu \rangle = 140$	$\langle \mu \rangle = 20$
Center of mass energy	$\sqrt{s} = 14 \text{ TeV}$	$\sqrt{s} = 8 \text{ TeV}$

Table 1.2: Expected running values for the Phase II HL-upgraded LHC with older values for comparison [21].

- 437 Where it should be noted that the integrated luminosity indicates the total amount
 438 of data which will be collected after the upgrade is completed before the next up-
 439 grade takes place.

440 1.3.8 Monte Carlo simulation

- 441 As mentioned before, in this thesis only emulated data has been used. This data
 442 is created by using a Monte Carlo simulation of the background processes and
 443 the expected signal. To do this a program called MadGraph is used.
 444 MadGraph [22] starts with Feynman diagrams and then generates simulated events
 445 based on lots of different parameters.
 446 PYTHIA [23] is a package which adds the correct description of jets to MadGraph
 447 by including hadronization. The correct description of pile-up comes from other
 448 ATLAS software.
 449 The tool to access all this data and analyse it a tool called ROOT, which is used
 450 for programming high energy physics related tools [24].

2

Validation of smearing functions

453 A full detector simulation of the ATLAS detector based on the GEANT [25] pro-
454 gram makes it possible to obtain the expected detector responses to electrons,
455 muons, tau leptons, photons (γ) and jets of hadrons. However these simulations
456 are extremely time-consuming and require a lot of computing power. Also at the
457 present time only a limited set of these simulations exists for the ATLAS phase II
458 upgrade.

459 In this thesis a different strategy is used. Instead of performing a full detector
460 simulation the observed particles from the event generator, which simulates the
461 proton-proton collisions, are smeared by using random numbers following reso-
462 lution functions specific to each type of particle. These emulate how the detector
463 and the reconstruction is affected by the increased luminosity and the pile-up
464 which comes with this.

465 The resolution functions or smearing functions are the official functions devel-
466 oped from previous studies [1, 26] by the ATLAS collaboration for the study of
467 the ATLAS phase II upgrade. The key feature of those studies was that the di-
468 rection of the momenta is unaffected and that only jets and E_T^{Miss} are affected by
469 pile-up. Since this was confirmed in previous studies it was not incorporated into
470 the smearing functions as discussed more in section 2.1.

471 Since part of this thesis work was to take the official ATLAS smearing functions
472 and apply the smearing to each particle, it was important to check that the en-
473 ergy and momenta resolutions of the smeared objects were consistent with the
474 expected values. Thus in this chapter the energy and momenta resolutions are
475 measured after applying the smearing to some simulated processes and the re-
476 sulting resolutions are compared with the expected values.

477 2.1 Smearing functions

478 These smearing functions are designed so that they take into account the effi-
479 ciency of the different detectors, limitations as well as their dependence on pile-
480 up. They also take into account how all this varies depending on the measured
481 entries energy or momenta.

482 Terminology:

- 483 • Data before smearing, simulated data, is denoted as data at a truth level or
484 truth data.
- 485 • Data after smearing, which is comparable to what is measured is denoted
486 as reconstructed or reco data as discussed in subsection 1.3.4.

487 2.1.1 Electron and photon

488 The identification of electrons relies on finding an isolated electron track and
489 a pattern in the calorimeter compatible with an electron shower. Pile-up will
490 affect the electrons by decreasing the efficiency to identify an electron because of
491 the increased number of tracks. However for the identified electrons the energy
492 resolution will be close to that without pile-up.

493 The electron and photon have the same smearing since they are both detected in
494 a similar way.

495 2.1.2 Muon

496 The identification of muons relies on isolated tracks in the inner detector being
497 matched with information in the muon system. Since the muon system is the
498 outer most detector seen from the collision point it is unaffected by the false
499 detection effects of pile-up.

500 2.1.3 Tau

501 Tau is detected similarly to electron and photon. In this thesis all tau processes
502 are assumed to be at 3 prong. Where prong refers to the different amount of
503 tracks from which they were reconstructed. This in turn means that the effect of
504 pile-up will be worse compared to an electron as a triplet must be found in an
505 increased number of tracks.

506 2.1.4 Jets

507 The largest effect of pile-up is to add additional jets in the ATLAS detector. These
508 additional jets contribute to additional energy deposited inside the existing jets
509 and to E_T^{Miss} .

510 2.1.5 Missing Transversal Energy

511 E_T^{Miss} , the missing transversal energy, which was discussed in subsection 1.3.6,
512 and defined in (1.9) is calculated by knowing that there should be energy conser-

513 vation in the collision. It is comprised of different parts, one from neutrinos, one
514 from errors in the other measurements and one from new physics. It should be
515 affected by pile-up as described above.

516 2.2 Validation

517 To validate the smearing functions a comparison with Ref. [26] was made where
 518 the standard deviation, depending on the energy or momentum value of an entity,
 519 was given, see section 2.4. This is performed using the simulated processes listed
 in table 2.1.

Table 2.1: Different processes from where data has been taken. Each sample is a simulation of a physical process, the simulation names can be found in appendix A

Particle	Process
Electron	$W \rightarrow e\nu$
Muon	$W \rightarrow \mu\nu$
Tau	$W \rightarrow \tau\nu$
γ	$\gamma + \text{Jet sample}$
Jets	Jet sample
E_T^{Miss}	$Z \rightarrow \nu\nu + \text{Jet sample}$

520
 521 The energy and momentum resolutions are obtained for each type of particle by
 522 comparing the values before and after smearing. This is done looking at the reco
 523 data for a given truth energy or momentum value. Since the smearing functions
 524 takes a lot into account the match will not be a fine line as seen in figure 2.3b.

525 By fitting a Gaussian curve to this data will then result in the standard deviation
 526 which is used in the validation. The standard deviation is also known as the
 527 resolution of the data and will be denoted σ .

528 This resolution is then compared to previous results, [26].

529 To get enough statistics enough data must be available for a given truth energy
 530 or momenta and the analysis must be specific enough to only look at a narrow
 531 enough interval around this point.

532 **2.3 Results**

- 533 As discussed above, the method was to plot the data against its smeared counter-
534 part and through this determine σ to see if it conforms to the expected values.
- 535 Only one energy value is shown for simplicity, though the comparison was done
536 for different energy values.
- 537 The average number of pile-up is fixed at 60 as a benchmark unless anything else
538 is stated.
- 539 The images are, as the comparison, often divided depending on the different η
540 values.
- 541 All results are summarized in table 2.5.

542 2.3.1 Electron and photon

543 Since these interact very similarly in the detector, their smearing functions are
 544 identical. The slice value represents at which value of unsmeared energy or mo-
 545 mentum this smearing occurs.

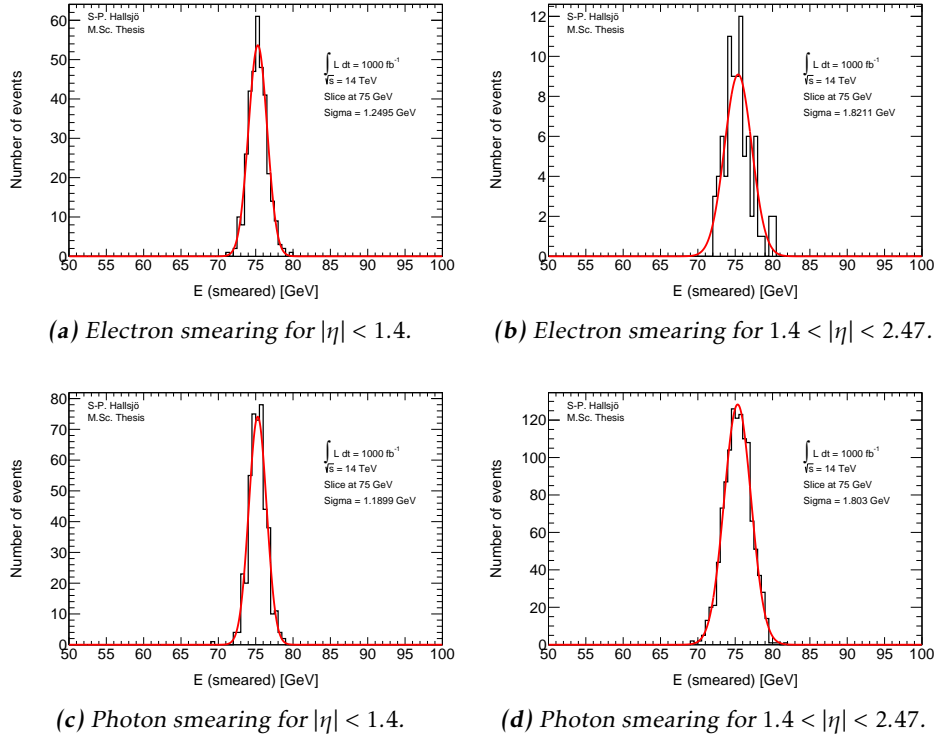


Figure 2.1: Photon and electron smearing plots.

546 **2.3.2 Muon**

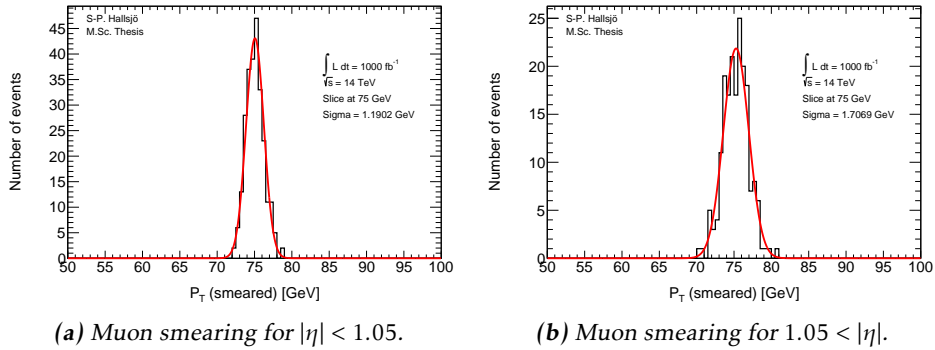


Figure 2.2: Muon smearing plots.

547 **2.3.3 Tau**

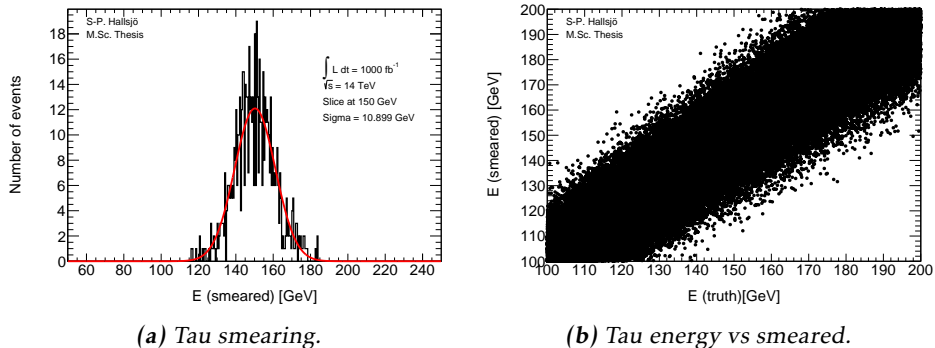


Figure 2.3: Tau smearing and energy vs smearing plot.

2.3.4 Jets

Jets as described in subsection 1.3.6, are hadronic showers. The smearing functions are divided into four different regions depending on the angle η .

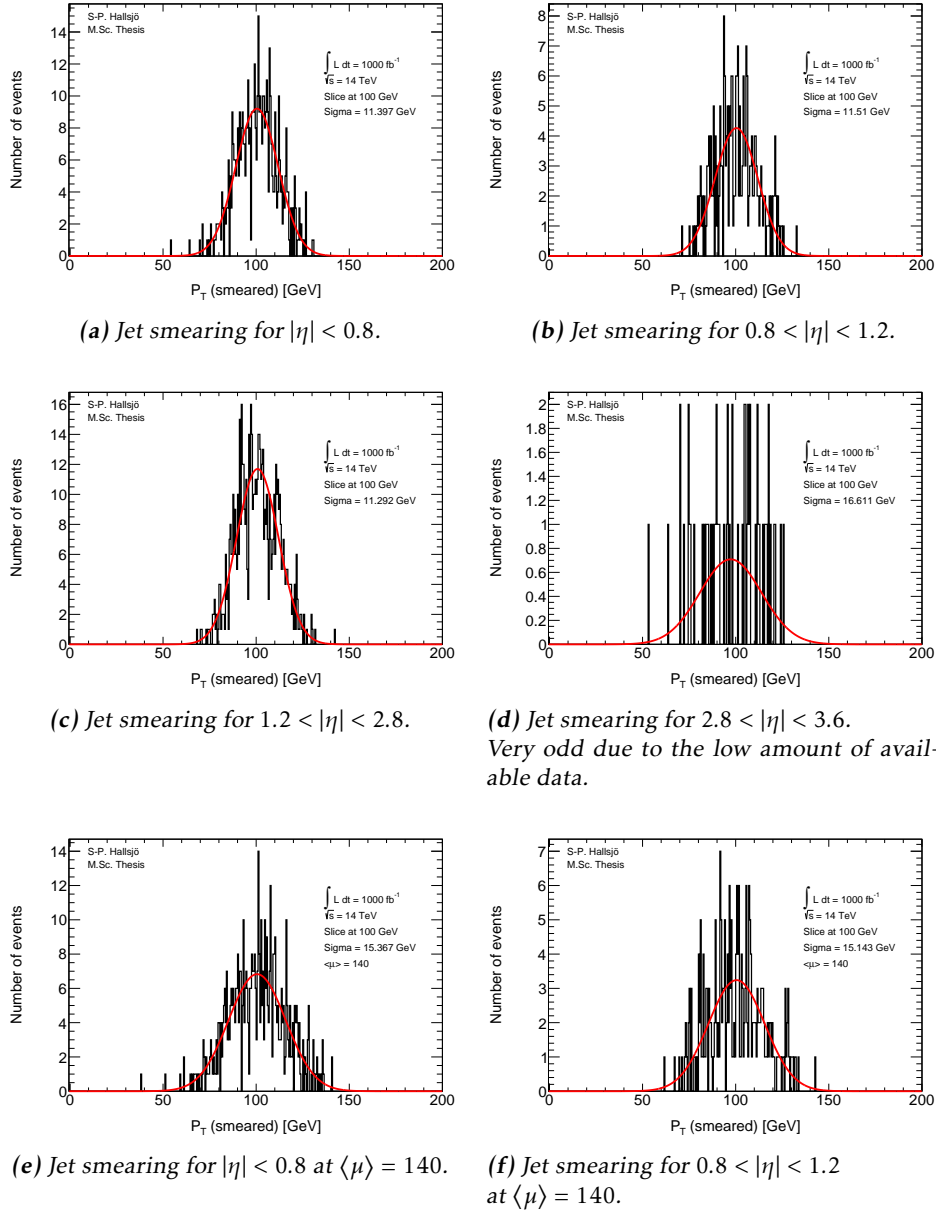


Figure 2.4: Jet smearing plots.

2.3.5 Missing Transversal Energy

These figures are given as smeared value from origin, thus at 0 it represents that the energy is unsmeared, compared to the others where the slice value represents the unsmeared.

Here the E_T^{Miss} is projected down to the x- and y-axis, since these are the transversal axes, to be smeared.

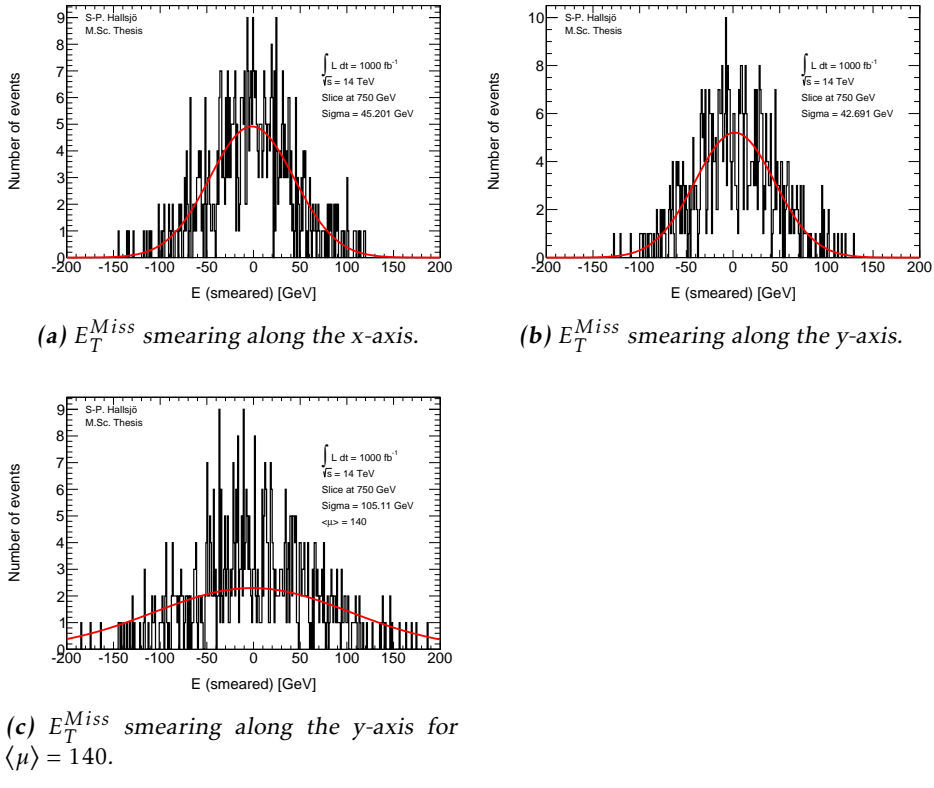


Figure 2.5: E_T^{Miss} smearing plots

2.4 Expected results

557 The expected response has been calculated and taken from [26].

559 The independence of pile-up for leptons and photons is backed up in previous
560 research, for instance [1, 27] were the first states:

561 “The uncertainty due to pile-up was investigated by comparing
562 simulated MC samples with and without pile-up and was found to be
563 negligible”

564 To validate the smearing code comparisons were made with [26] which gave the
565 following formulation for the expected σ :

Observable	Absolute σ
Electron & photon	$\sigma = 0.3 \oplus 0.1\sqrt{E(GeV)} \oplus 0.01E(GeV), \eta < 1.4$ $\sigma = 0.3 \oplus 0.15\sqrt{E(GeV)} \oplus 0.015E(GeV), 1.4 < \eta < 2.47$
Muon momentum	$\sigma = \frac{\sigma_{id}\sigma_{ms}}{\sigma_{id} \oplus \sigma_{ms}}$ $\sigma_{id} = P_T(a_1 \oplus a_2 P_T)$ $\sigma_{ms} = P_T(\frac{b_0}{P_T} \oplus b_1 \oplus b_2 P_T)$
Tau energy	$\sigma = (0.03 \oplus \frac{0.76}{\sqrt{E(GeV)}})E(GeV)$, for 3 prong.
Jet momentum	$\sigma = P_T(GeV)(\frac{N}{P_T} \oplus \frac{S}{\sqrt{P_T}} \oplus C)$ where $N = a(\eta) + b(\eta)\mu$
E_T^{Miss}	$\sigma = (0.4 + 0.09\sqrt{\mu})\sqrt{\sum E(GeV) + 20\mu}$

Table 2.2: Expected absolute σ where the parameters are given for muons in table 2.3 and for jets in table 2.4. Functions take from [26].

	a_1	a_2	b_0	b_1	b_2
$ \eta < 1.05$	0.01607	0.000307	0.24	0.02676	0.00012
$ \eta > 1.05$	0.03000	0.000387	0.00	0.03880	0.00016

Table 2.3: Parameters used in the muon smearing function taken from [26].

$ \eta $	a	b	s	C
0-0.8	3.2	0.07	0.74	0.05
0.8-1.2	3.0	0.07	0.81	0.05
1.2-2.8	3.3	0.08	0.54	0.05
2.8-3.6	2.8	0.11	0.83	0.05

Table 2.4: Parameters used in the jet smearing function taken from [26].

Process	σ [GeV]	Expected σ
Electron low η	1.24948 ± 0.0481987	1.18427
High η	1.8211 ± 0.141329	1.74446
Photon low η	1.18986 ± 0.0400187	1.18427
High η	1.80297 ± 0.0374312	1.744463
Muon low η	1.19016 ± 0.0524938	1.49789
High η	1.70694 ± 0.0882606	2.18318
Tau	10.8992 ± 0.299761	10.3388
Jet low η	11.3974 ± 0.351391	11.5983
$\langle \mu \rangle = 140$	15.3673 ± 0.473783	15.7721
Mid low η	11.5096 ± 0.518872	11.9352
$\langle \mu \rangle = 140$	15.1427 ± 0.682649	15.9515
Mid high η	11.2916 ± 0.310314	10.9439
High η	16.6112 ± 1.52891	13.5
E_T^{Miss} x-axis	45.2013 ± 1.35426	48.4483
E_T^{Miss} y-axis	42.6906 ± 2.27904	48.44834
$\langle \mu \rangle = 140$	105.109 ± 12.239	87.2812

Table 2.5: σ values.

- 566 • Where the given σ is still the absolute.
- 567 • Where the large difference between calculated and expected σ for Muons
568 and E_T^{Miss} is explained by incorrectly calculated errors in σ .

569 2.5 Discussion

570 2.5.1 Smearing independent on pile-up

571 From the validation done it was interesting to note that the smearing functions
572 were created from previous studies, [1, 27], which had shown that leptons and
573 photons are not affected by pile-up. This may seem incredible however it be-
574 comes quite logical when one understands how the detectors work. To be able to
575 detect particles the detectors must detect an excess of energy which comes from
576 a particle passing through. This should not be distorted by an increased pile-up.
577 The amount of particles passing through will of course increase, but the detec-
578 tions should be unaffected as well as the recreation of the events. However with
579 the same logic it makes sense that jets and E_T^{Miss} are quite affected since they
580 are combined of several parts, either hadronic particles or by all the transversal
581 missing energy.

582 Another interesting part is how the effect diminishes with and increasing energy.
583 As seen above, and through the the formula, for the high energies which were of
584 interest here the effect is minimal.

585 2.5.2 Comparison to expected results

586 One of the major problems in the comparison was to get the significance of the
587 Gaussian fit to be calculated correctly. The tool ROOT has a lot of different fea-
588 tures which made this task somewhat difficult. Also since this is a statistical
589 property there is a statistical fluctuation in the result.

590 Another was to retrieve the correct values from the paper, [26], since it was un-
591 clear if the values given were absolute or scale dependent. This has now been
592 corrected in a new version of the paper.

593 **2.6 Conclusion**

- 594 The smearing functions work as intended within 5.8 sigma, however when using
595 a test box and averaging the sigmas one ends up with half of this for the extreme
596 cases, muons and E_T^{Miss} y-axis.

3

Evaluating dark matter signals

599 The main goal of the thesis is to investigate if certain dark matter signals can
600 be detected after the high luminosity upgrade. One immediate worry is that the
601 background will be large in comparison to the signal, making the signal unde-
602 tectable.

603 The following signals models have been used: The signal models are given in
604 appendix A along with the background. The different models were discussed in
605 part in subsection 1.2.5 and some more in this chapter.

606 Each of these has been evaluated in different signal regions and the detectability
607 has been evaluated using a statistical P-value. This process has been performed
608 at different pile-up values.

609 **What background existed? How was it simulated in MC? Should that be here**
610 **or in appendix?**

611 Dont mention, but good to know. Used METpt in all histograms, with the weight
612 as in main.C and mainclass.C.

613 3.1 Signal to background ratio

614 What I am doing now, looking at what signal? What are the different background
615 processes? What and why was the weight used?

616 Signals should be explained somewhat in the introduction.

617 Look at presentation, is it worth bringing up the first signal regions when the
618 data has already been filtered? Should that be here?

619 3.1.1 Selection criteria

620 What criteria were used and more importantly why? It is quite important that
 621 you can explain why this was used.

622 For different purposes different selection criteria or regions are used. These are a
 623 set of criteria specified to enhance the area of interest. For instance, if simulating
 624 a specific signal one wants to find as many ways as possible to diminish the back-
 625 ground. This so that when searching experimentally, the signal will be easier to
 626 detect.

627 These can be quite general cuts, there are only some things to take into consider-
 628 ation.

- 629 • If experimental, what limitations are set by the detectors? Are there some
 630 criteria already?
- 631 • If simulated, is there some criteria set in the generator?
- 632 • Are there criteria which must be set since there is to much uncertainty in
 633 the data? or a large effect of pile up?

634 3.1.2 Verifying background data

635 To verify that the background data was correct it was compared with [28], in
 636 which the luminosity if 10 fb^{-1} and thus the expected values from the paper
 637 scaled up with a factor 100. **Also, somewhat unexpectedly is that the differ-
 ence in center of mass energy required the cross-sections to be much lowered
 than compared with the upgrade.** The signal region used in the article were the
 639 following:

Selection Criteria		
Jet veto, require no more than 2 jets with $p_T > 30 \text{ GeV}$ and $ \eta < 4.5$		
Lepton veto, no electron or muon		
Leading jet with $ \eta < 2.0$ and $\Delta\phi(\text{jet}, E_T^{\text{Miss}}) > 0.5$ (second-leading jet)		
signal region	SR3p	SR4p
minimum leading jet p_T (GeV)	350	500
minimum E_T^{Miss} (GeV)	350	500

Table 3.1: The signal regions

640
 641 The article has several different signal regions, the difference is the last item, un-
 642 fortunately since the simulated events are already filtered before the analysis only
 643 one of the regions could be used.

644 NEW WITH 350 as SR3 and 500 as SR4 and expected (Scaled to 1000 fb^{-1}) thus
 645 scaled a factor 100 since luminosity is only a measurement of the amount of data
 646 and does not change anything physical.

Process	SR3p	Expected SR3p	SR4p	Expected SR4p
$Z \rightarrow \nu\nu$	140298	152000	25250.3	27000
$W \rightarrow \tau\nu$	40700.8	37000	5861.74	3900
$W \rightarrow e\nu$	11229	11200	1506.58	1600
$W \rightarrow \mu\nu$	13727.1	15800	1872.32	4200
Total background	205955	218000	34491	36700

Table 3.2: Comparison of the simulated and expected events from [28].

In table 3.2 a comparison has been made. It can be seen that the simulated events and expected events coincide on all accounts apart from $W \rightarrow \tau\nu$, $W \rightarrow \mu\nu$ and thus the total as well. **This can be explained by better separation of μ, τ and missing energy.** Tau can not be reconstructed as jets in the code, they can in reality!

3.1.3 Figures of merit

P-value, info from Majas phd thesis. Is there a source? Should there be a figure?

To be able to evaluate different signal regions and different signal models, a figure of merit p is used. The value p is the probability for an assumed hypothesis to be correct, thus a good signal region will yield a low value. The assumed hypothesis is that the background and its fluctuations is measured over the signal plus background.

Assuming the expected number of background events are $B \pm \sigma_B$ where σ_B is the quadratic sum of the statistical error from Monte Carlo, the statistical error from the control region and the systematic errors. The expected number of signals is S, assumed without fluctuation.

If no uncertainty in B or S is assumed, then the number of expected events, N, in the signal region should follow a Poisson distribution as such:

$$P(N|S+B) = \frac{e^{-(S+B)}(S+B)^N}{N!} \quad (3.1)$$

However since there is an uncertainty in the background, the probability distribution $P(N|S+B)$ must be convoluted with a Gaussian function:

$$G(N_B|B, \sigma_B) = \frac{1}{\sigma_B \sqrt{2\pi}} e^{-\frac{(N_B-B)^2}{2\sigma_B^2}} \quad (3.2)$$

where N_B is the expected number of background events. The convolution is done

using N_B as N resulting in the total probability density function:

$$\begin{aligned} F(N|S+B, \sigma_B) &= P(N|S+N_B)*G(N_B|B, \sigma_B) = \\ &= \int_{-\infty}^{\infty} P(N|N_B - (S + B))G(N_B|B, \sigma_B)dN_B \end{aligned} \quad (3.3)$$

668 This leads to the probability of the signal plus background fluctuation to B events
 669 being obtained by summing the probability function from $N=0$ to $N=B$.

$$p = \sum_{i=0}^B \int_{-\infty}^{\infty} P(i|N_B - (S+B))G(N_B|B, \sigma_B)dN_B \quad (3.4)$$

670 3.1.4 D5 operators

671 Discuss M^* , and the difference in mDM. From presentation given, 3-4 April.

672 Was discussed in part in subsection 1.2.5

673 As described in the introduction **reference?**, one of the signals is modelled using
 674 the D5 operator. In this thesis two different scenarios were used, one at a dark
 675 matter mass of 50 GeV and one at 400 GeV.

676 3.1.5 Light vector mediator models

677 Discuss M_m , width, and the difference in mDM. From presentation given, 3-4
 678 April.

679 Was discussed in part in subsection 1.2.5

680 As described in the introduction **reference?**, the other signal model is a vector
 681 mediator model. The data available is: two different widths $M/3$ and $M/8\pi$.
 682 **M?!**? two different mDM, 50 GeV and 400 GeV and finally a variety of mediator
 683 masses.

684 3.1.6 Susy models?

685 3.2 Other selection criteria and observables

686 New signal regions.

687 3.3 Mitigating the effect of the high luminosity

688 Something pile-up Something as seen in validation of... the effect is quite minute
 689 for high energy values and does not at all affect leptons or photons. Mention that
 690 the effect is on a trigger level, that the lowest SR will be lost.

691 Even though this was envisioned as the primary focus of the thesis, it was shown
 692 that the effect of pile-up is minute for these high signal regions. Thus the focus

Selection Criteria

Jet veto, require no more than 2 jets with $p_T > 30\text{GeV}$ and $|\eta| < 4.5$

Lepton veto, no electron or muon

Leading jet with $|\eta| < 2.0$ and $\Delta\phi(\text{jet}, E_T^{\text{Miss}}) > 0.5$ (second-leading jet)

signal region	SR0	SR1	SR2	SR3	SR4
minimum leading jet p_T (GeV)	120	350	600	800	1000
minimum E_T^{Miss} (GeV)	120	350	600	800	1000
signal region	SR0	SRa	SRb	SRc	SRd
minimum leading jet p_T (GeV)	350	350	350	350	350
minimum E_T^{Miss} (GeV)	120	350	600	800	1000

Table 3.3: The new signal regions

693 was shifted to perform a more in-depth mono-jet analysis of different DM signal
694 models.

695 3.4 Results

696 3.4.1 Limit on M^*

697 The mass suppression scale. Give at 1000fb^{-1} . And for the different signal re-
698 gions. **ASK CHRISTOPHE FOR A GOOD EXPLANATION OF M^* and why**
699 **there can be limits!**

700 For the new signal regions: **Include a table of the limits for truth and Reco.**

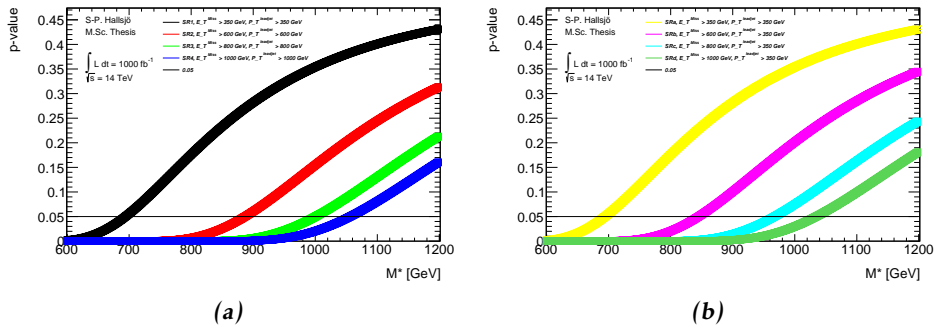


Figure 3.1: On a truth level.

701 3.4.2 Effect of pile-up on M^*

702 Hardly any effect. 10 % or in that vicinity.

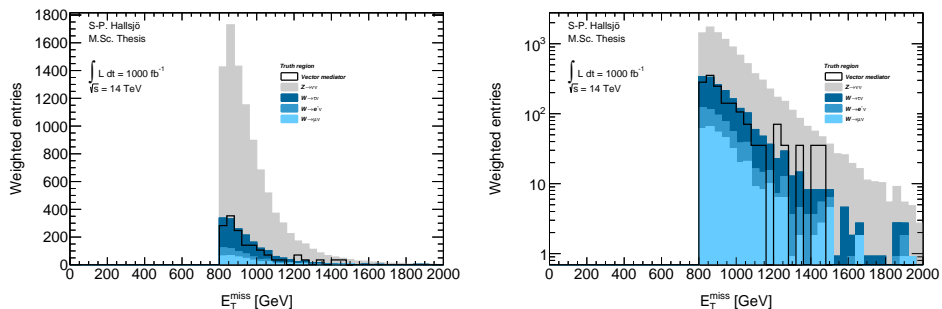
3.4.3 Previous results

Valerios paper for instance. Preliminary note that much better results for 1000fb-1 and 14TeV.

The whole discussion with Steven and David.

3.4.4 Limit on mediator mass

Are there previous results? Signal vs background plot in normal and log scale for one of the vector mediator models, to be able to evaluate all the different models the so called p-value was used in different signal regions. Below are two figures showing one of the vector mediator models in SR3.



(a) Signal on background plot for E_T^{Miss} on reco level in SR3. (b) The same as a) with log scale on the y-axis

Figure 3.2: Signal on background plot to illustrate the a general plot.

To set a limit on the mediator mass the p-value was calculated in different signal regions for the different signal models with different mediator mass. This resulted in the following plot:

3.4.5 Effect of pile-up on mediator mass

Check the different cases for reco and truth to see what happens.

3.5 Discussion

3.6 Conclusion

4

Results and Conclusions

721 4.1 Validation of smearing functions

722 Have some discussion.

723 Result they appear to work as expected, the reference paper was a bit unclear, I
724 leave my writing as a better reference.

725 4.2 Signal to background ratio

726 4.2.1 Limit on M^*

727 4.2.2 Limit on mediator mass

728 4.3 Other selection criteria and observables

729 4.3.1 Limit on M^*

730 4.3.2 Limit on mediator mass

731 4.4 Mitigating the effect of the high luminosity

732 4.5 Recommendations to mitigate the effect of the 733 high luminosity

734 Keep to a higher energy region, or signal region.

735 4.6 Suggestions for future research

736 With more time, search for new signal regions, the only solution now for the HL
737 is to go up in energy. Since none of the other parameters (eta,phi etc) seem to be
738 altered these can not be used. Is there something that has been overlooked?

739 Test the effect of pile-up for lower signal regions? See if the effect is as great as
740 predicted.

741 Explore other theoretical models for dark matter, other d operators etc. Models
742 that are based on Supersymmetry and not just effective theories.

743 Sätt av ett kort kapitel sist i rapporten till att avrunda och föreslå räkningar för
744 framtida utveckling av arbetet.

745 Saving as reference. test citing as: Here we cite Duck [29] [29].

746 If the above works, remember to edit myreferences.

Appendix

A

Datasets

750 **A.1 Background processes**

751 **A.1.1 Validation**

752 For the validation the following datasets were used, with a filter at generator level
 753 at 450GeV for lead jet and MET.

754 mc12.157539.sherpa_ct10_znunupt280d4pd.v03 mc12.157534.sherpa_ct10_wenupt200d4pd.v03

755 mc12.157535.sherpa_ct10_wmunupt200d4pd.v03

756 mc12.157536.sherpa_ct10_wtaunupt200d4pd.v03

757 mc12.129160.pythia8_au2cteq6l1_perf_jf17d4pd.v03

758 mc12.129160.pythia8_au2cteq6l1_perf_jf17d4pd.v04

759 mc12.129170.pythia8_au2cteq6l1_gammajet_dp17d4pd.v04

760 They should be read as such: Monte Carlo version, dataset number, generator, ?
 761 name.

763 **A.1.2 Background to signals**

764 The same as the above though now with the filter as indicated by their name. The
 765 second znunu sample has been generated with and center of mass energy at 8
 766 TeV.

767 mc12.157539.sherpa_ct10_znunupt280d4pd.v05

768 mc12.157539.8tev_sherpa_ct10_znunupt280d4pd.v05

769 mc12.157536.sherpa_ct10_wtaunupt200d4pd.v05

770 mc12.157534.sherpa_ct10_wenupt200d4pd.v05

771 mc12.157535.sherpa_ct10_wmunupt200d4pd.v05

772 A.2 D5 signal processes

```

773 mc12.188408.madgraphpythia_auet2bcteq6l1_d5_dm50_ms10000_
774 qcut200d4pd.v06
775 mc12.188409.madgraphpythia_auet2bcteq6l1_d5_dm50_ms10000_
776 qcut400d4pd.v06
777 mc12.188410.madgraphpythia_auet2bcteq6l1_d5_dm50_ms10000_
778 qcut600d4pd.v06

779 mc12.188411.madgraphpythia_auet2bcteq6l1_d5_dm400_ms10000_
780 qcut200d4pd.v06
781 mc12.188412.madgraphpythia_auet2bcteq6l1_d5_dm400_ms10000_
782 qcut400d4pd.v06
783 mc12.188413.madgraphpythia_auet2bcteq6l1_d5_dm400_ms10000_
784 qcut600d4pd.v06

```

785 All signals should be read as such: Monte Carlo version, dataset number, genera-
 786 tor, ?, name of operator, dark matter mass, default mass suppression scale,
 787 qcut part. As discussed in **reference**
 788 qcut means that the original data has been split into different parts depending on
 789 the value of the lead jet pt.

790 A.3 Light vector mediator processes

```

791 mc12.188414.madgraphpythia_auet2bcteq6l1_dmv_dm50_mm100_w3_
792 qcut200d4pd.v06
793 mc12.188422.madgraphpythia_auet2bcteq6l1_dmv_dm50_mm100_w3_
794 qcut400d4pd.v06
795 mc12.188430.madgraphpythia_auet2bcteq6l1_dmv_dm50_mm100_w3_
796 qcut600d4pd.v06

797 mc12.188415.madgraphpythia_auet2bcteq6l1_dmv_dm50_mm300_w3_
798 qcut200d4pd.v06
799 mc12.188423.madgraphpythia_auet2bcteq6l1_dmv_dm50_mm300_w3_
800 qcut400d4pd.v06
801 mc12.188431.madgraphpythia_auet2bcteq6l1_dmv_dm50_mm300_w3_
802 qcut600d4pd.v06

803 mc12.188416.madgraphpythia_auet2bcteq6l1_dmv_dm50_mm500_w3_
804 qcut200d4pd.v06
805 mc12.188424.madgraphpythia_auet2bcteq6l1_dmv_dm50_mm500_w3_
806 qcut400d4pd.v06
807 mc12.188432.madgraphpythia_auet2bcteq6l1_dmv_dm50_mm500_w3_
808 qcut600d4pd.v06

809 mc12.188417.madgraphpythia_auet2bcteq6l1_dmv_dm50_mm1000_w3_
810 qcut200d4pd.v06
811 mc12.188425.madgraphpythia_auet2bcteq6l1_dmv_dm50_mm1000_w3_

```

```
812 qcut400d4pd.v06
813 mc12.188433.madgraphpythia_auet2bcteq6l1_dmv_dm50_mm1000_w3_
814 qcut600d4pd.v06
815 mc12.188418.madgraphpythia_auet2bcteq6l1_dmv_dm50_mm3000_w3_
816 qcut200d4pd.v06
817 mc12.188426.madgraphpythia_auet2bcteq6l1_dmv_dm50_mm3000_w3_
818 qcut400d4pd.v06
819 mc12.188434.madgraphpythia_auet2bcteq6l1_dmv_dm50_mm3000_w3_
820 qcut600d4pd.v06
821 mc12.188419.madgraphpythia_auet2bcteq6l1_dmv_dm50_mm6000_w3_
822 qcut200d4pd.v06
823 mc12.188427.madgraphpythia_auet2bcteq6l1_dmv_dm50_mm6000_w3_
824 qcut400d4pd.v06
825 mc12.188435.madgraphpythia_auet2bcteq6l1_dmv_dm50_mm6000_w3_
826 qcut600d4pd.v06
827 mc12.188420.madgraphpythia_auet2bcteq6l1_dmv_dm50_mm10000_w3_
828 qcut200d4pd.v06
829 mc12.188428.madgraphpythia_auet2bcteq6l1_dmv_dm50_mm10000_w3_
830 qcut400d4pd.v06
831 mc12.188436.madgraphpythia_auet2bcteq6l1_dmv_dm50_mm10000_w3_
832 qcut600d4pd.v06
833 mc12.188421.madgraphpythia_auet2bcteq6l1_dmv_dm50_mm15000_w3_
834 qcut200d4pd.v06
835 mc12.188429.madgraphpythia_auet2bcteq6l1_dmv_dm50_mm15000_w3_
836 qcut400d4pd.v06
837 mc12.188437.madgraphpythia_auet2bcteq6l1_dmv_dm50_mm15000_w3_
838 qcut600d4pd.v06
839 mc12.188438.madgraphpythia_auet2bcteq6l1_dmv_dm50_mm100_w8pi_
840 qcut200d4pd.v06
841 mc12.188446.madgraphpythia_auet2bcteq6l1_dmv_dm50_mm100_w8pi_
842 qcut400d4pd.v06
843 mc12.188454.madgraphpythia_auet2bcteq6l1_dmv_dm50_mm100_w8pi_
844 qcut600d4pd.v06
845 mc12.188439.madgraphpythia_auet2bcteq6l1_dmv_dm50_mm300_w8pi_
846 qcut200d4pd.v06
847 mc12.188447.madgraphpythia_auet2bcteq6l1_dmv_dm50_mm300_w8pi_
848 qcut400d4pd.v06
849 mc12.188455.madgraphpythia_auet2bcteq6l1_dmv_dm50_mm300_w8pi_
850 qcut600d4pd.v06
851 mc12.188440.madgraphpythia_auet2bcteq6l1_dmv_dm50_mm500_w8pi_
852 qcut200d4pd.v06
853 mc12.188448.madgraphpythia_auet2bcteq6l1_dmv_dm50_mm500_w8pi_
```

```
854 qcut400d4pd.v06
855 mc12.188456.madgraphpythia_auet2bcteq6l1_dmv_dm50_mm500_w8pi_
856 qcut600d4pd.v06
857 mc12.188441.madgraphpythia_auet2bcteq6l1_dmv_dm50_mm1000_w8pi_
858 qcut200d4pd.v06
859 mc12.188449.madgraphpythia_auet2bcteq6l1_dmv_dm50_mm1000_w8pi_
860 qcut400d4pd.v06
861 mc12.188457.madgraphpythia_auet2bcteq6l1_dmv_dm50_mm1000_w8pi_
862 qcut600d4pd.v06
863 mc12.188442.madgraphpythia_auet2bcteq6l1_dmv_dm50_mm3000_w8pi_
864 qcut200d4pd.v06
865 mc12.188450.madgraphpythia_auet2bcteq6l1_dmv_dm50_mm3000_w8pi_
866 qcut400d4pd.v06
867 mc12.188458.madgraphpythia_auet2bcteq6l1_dmv_dm50_mm3000_w8pi_
868 qcut600d4pd.v06
869 mc12.188444.madgraphpythia_auet2bcteq6l1_dmv_dm50_mm10000_w8pi_
870 qcut200d4pd.v06
871 mc12.188452.madgraphpythia_auet2bcteq6l1_dmv_dm50_mm10000_w8pi_
872 qcut400d4pd.v06
873 mc12.188460.madgraphpythia_auet2bcteq6l1_dmv_dm50_mm10000_w8pi_
874 qcut600d4pd.v06
875 mc12.188445.madgraphpythia_auet2bcteq6l1_dmv_dm50_mm15000_w8pi_
876 qcut200d4pd.v06
877 mc12.188453.madgraphpythia_auet2bcteq6l1_dmv_dm50_mm15000_w8pi_
878 qcut400d4pd.v06
879 mc12.188461.madgraphpythia_auet2bcteq6l1_dmv_dm50_mm15000_w8pi_
880 qcut600d4pd.v06
881 mc12.188462.madgraphpythia_auet2bcteq6l1_dmv_dm400_mm500_w3_
882 qcut200d4pd.v06
883 mc12.188468.madgraphpythia_auet2bcteq6l1_dmv_dm400_mm500_w3_
884 qcut400d4pd.v06
885 mc12.188474.madgraphpythia_auet2bcteq6l1_dmv_dm400_mm500_w3_
886 qcut600d4pd.v06
887 mc12.188463.madgraphpythia_auet2bcteq6l1_dmv_dm400_mm1000_w3_
888 qcut200d4pd.v06
889 mc12.188469.madgraphpythia_auet2bcteq6l1_dmv_dm400_mm1000_w3_
890 qcut400d4pd.v06
891 mc12.188475.madgraphpythia_auet2bcteq6l1_dmv_dm400_mm1000_w3_
892 qcut600d4pd.v06
893 mc12.188464.madgraphpythia_auet2bcteq6l1_dmv_dm400_mm3000_w3_
894 qcut200d4pd.v06
895 mc12.188470.madgraphpythia_auet2bcteq6l1_dmv_dm400_mm3000_w3_
```

```
896 qcut400d4pd.v06
897 mc12.188476.madgraphpythia_auet2bcteq6l1_dmv_dm400_mm3000_w3_
898 qcut600d4pd.v06
899 mc12.188465.madgraphpythia_auet2bcteq6l1_dmv_dm400_mm6000_w3_
900 qcut200d4pd.v06
901 mc12.188471.madgraphpythia_auet2bcteq6l1_dmv_dm400_mm6000_w3_
902 qcut400d4pd.v06
903 mc12.188477.madgraphpythia_auet2bcteq6l1_dmv_dm400_mm6000_w3_
904 qcut600d4pd.v06
905 mc12.188466.madgraphpythia_auet2bcteq6l1_dmv_dm400_mm10000_w3_
906 qcut200d4pd.v06
907 mc12.188472.madgraphpythia_auet2bcteq6l1_dmv_dm400_mm10000_w3_
908 qcut400d4pd.v06
909 mc12.188478.madgraphpythia_auet2bcteq6l1_dmv_dm400_mm10000_w3_
910 qcut600d4pd.v06
911 mc12.188467.madgraphpythia_auet2bcteq6l1_dmv_dm400_mm15000_w3_
912 qcut200d4pd.v06
913 mc12.188473.madgraphpythia_auet2bcteq6l1_dmv_dm400_mm15000_w3_
914 qcut400d4pd.v06
915 mc12.188479.madgraphpythia_auet2bcteq6l1_dmv_dm400_mm15000_w3_
916 qcut600d4pd.v06
917 mc12.188480.madgraphpythia_auet2bcteq6l1_dmv_dm400_mm500_w8pi_
918 qcut200d4pd.v06
919 mc12.188486.madgraphpythia_auet2bcteq6l1_dmv_dm400_mm500_w8pi_
920 qcut400d4pd.v06
921 mc12.188492.madgraphpythia_auet2bcteq6l1_dmv_dm400_mm500_w8pi_
922 qcut600d4pd.v06
923 mc12.188481.madgraphpythia_auet2bcteq6l1_dmv_dm400_mm1000_w8pi_
924 qcut200d4pd.v06
925 mc12.188487.madgraphpythia_auet2bcteq6l1_dmv_dm400_mm1000_w8pi_
926 qcut400d4pd.v06
927 mc12.188493.madgraphpythia_auet2bcteq6l1_dmv_dm400_mm1000_w8pi_
928 qcut600d4pd.v06
929 mc12.188482.madgraphpythia_auet2bcteq6l1_dmv_dm400_mm3000_w8pi_
930 qcut200d4pd.v06
931 mc12.188488.madgraphpythia_auet2bcteq6l1_dmv_dm400_mm3000_w8pi_
932 qcut400d4pd.v06
933 mc12.188494.madgraphpythia_auet2bcteq6l1_dmv_dm400_mm3000_w8pi_
934 qcut600d4pd.v06
935 mc12.188483.madgraphpythia_auet2bcteq6l1_dmv_dm400_mm6000_w8pi_
936 qcut200d4pd.v06
937 mc12.188489.madgraphpythia_auet2bcteq6l1_dmv_dm400_mm6000_w8pi_
```

```
938 qcut400d4pd.v06
939 mc12.188495.madgraphpythia_auet2bcteq6l1_dmv_dm400_mm6000_w8pi_
940 qcut600d4pd.v06
941 mc12.188484.madgraphpythia_auet2bcteq6l1_dmv_dm400_mm10000_w8pi_
942 qcut200d4pd.v06
943 mc12.188490.madgraphpythia_auet2bcteq6l1_dmv_dm400_mm10000_w8pi_
944 qcut400d4pd.v06
945 mc12.188496.madgraphpythia_auet2bcteq6l1_dmv_dm400_mm10000_w8pi_
946 qcut600d4pd.v06
947 mc12.188485.madgraphpythia_auet2bcteq6l1_dmv_dm400_mm15000_w8pi_
948 qcut200d4pd.v06
949 mc12.188491.madgraphpythia_auet2bcteq6l1_dmv_dm400_mm15000_w8pi_
950 qcut400d4pd.v06
951 mc12.188497.madgraphpythia_auet2bcteq6l1_dmv_dm400_mm15000_w8pi_
952 qcut600d4pd.v06
```

953

954

Bibliography

- [1] Collaboration ATLAS. Letter of Intent for the Phase-II Upgrade of the ATLAS Experiment. Dec 2012. URL <https://cds.cern.ch/record/1502664/>. Cited on pages 1, 17, 26, and 28.
- [2] B.H. Bransden and C.J. Joachain. *Quantum mechanics*. Pearson Education, second edition, 2000. Cited on page 3.
- [3] Sven-Patrik Hallsjö. Covering the sphere with noncontextuality inequalities. Bachelor's thesis, Linköping University, The Institute of Technology, 2013. URL [http://urn.kb.se/resolve?urn=urn:nbn:se:liu:diva-103663](http://urn.kb.se/resolve?urn=urn:nbn:se:liu.diva-103663). Cited on page 3.
- [4] A. Zee. *Quantum Field Theory in a Nutshell*. Princeton University Press, illustrated edition edition, March 2003. ISBN 0691010196. Cited on pages 3, 6, and 7.
- [5] Herbert Goldstein, Charles P. Poole, and John L. Safko. *Classical Mechanics (3rd Edition)*. Addison-Wesley, 3 edition, June 2001. ISBN 0201657023. Cited on page 3.
- [6] W. E. Burcham and M. Jobes. *Nuclear and Particle Physics*. Pearson education, second edition, 1995. Cited on page 4.
- [7] The ATLAS Collaboration. Observation of a new particle in the search for the Standard Model Higgs boson with the ATLAS detector at the LHC. *Phys. Lett. B*, 716(arXiv:1207.7214). CERN-PH-EP-2012-218):1–29. 39 p, Aug 2012. Cited on page 4.
- [8] Standard model of elementary particles. http://en.wikipedia.org/wiki/File:Standard_Model_of_Elementary_Particles.svg, 2014. Accessed: 2014-03-24. Cited on page 4.
- [9] G. Jungman, M. Kamionkowski, and K. Griest. Supersymmetric dark matter. *Physics Reports*, 267:195–373, March 1996. doi: 10.1016/0370-1573(95)00058-5. Cited on pages 4 and 5.

- [10] NASA. NASA's solar system exploration: the planets: orbits and physical characteristics. <https://solarsystem.nasa.gov/planets/charchart.cfm>, 2014. Accessed: 2014-03-21. Cited on page 6.
- [11] T. S. van Albada, J. N. Bahcall, K. Begeman, and R. Sancisi. Distribution of dark matter in the spiral galaxy NGC 3198. *Astrophysical Journal*, 295: 305–313, August 1985. doi: 10.1086/163375. Cited on page 6.
- [12] Jessica Goodman, Masahiro Ibe, Arvind Rajaraman, William Shepherd, Tim M.P. Tait, et al. Constraints on Light Majorana dark Matter from Colliders. *Phys.Lett.*, B695:185–188, 2011. doi: 10.1016/j.physletb.2010.11.009. Cited on pages 5 and 7.
- [13] ATLAS Collaboration. Search for dark matter candidates and large extra dimensions in events with a jet and missing transverse momentum with the atlas detector. *J. High Energy Phys.*, 04(arXiv:1210.4491. CERN-PH-EP-2012-210):075. 58 p, October 2012. URL <http://cds.cern.ch/record/1485031>. Cited on pages 5, 8, and 9.
- [14] J. Goodman, M. Ibe, A. Rajaraman, W. Shepherd, T. M. P. Tait, and H.-B. Yu. Constraints on dark matter from colliders. *Phys.Rev.D82:116010,2010*, 82(11):116010, December 2010. doi: 10.1103/PhysRevD.82.116010. Cited on page 7.
- [15] ATLAS. Atlas luminosity public results. <https://twiki.cern.ch/twiki/bin/view/AtlasPublic/LuminosityPublicResults>, 2013. Accessed: 2014-03-06. Cited on page 10.
- [16] AC Team. The four main LHC experiments, Jun 1999. URL <http://cds.cern.ch/record/40525>. Cited on page 10.
- [17] Werner Herr and B Muratori. Concept of luminosity. 2006. URL <http://cds.cern.ch/record/941318/>. Cited on page 11.
- [18] The ATLAS Collaboration. The atlas experiment at the cern large hadron collider. *Journal of Instrumentation*, 3(08):S08003. 437 p, 2008. URL <https://cdsweb.cern.ch/record/1129811/>. Cited on pages 11 and 12.
- [19] Joao Pequenao. Computer generated image of the whole ATLAS detector, Mar 2008. URL <http://cds.cern.ch/record/1095924>. Cited on page 12.
- [20] ATLAS Collaboration. Event display for one of the monojet candidates in the data. The event has a jet with $\text{pt} = 602 \text{ GeV}$ at $\eta = -1$ and $\phi = 2.6$, $\text{MET} = 523 \text{ GeV}$, and no additional jet with $\text{pt}_{\text{jet}} > 30 \text{ GeV}$ in the final state.. https://atlas.web.cern.ch/Atlas/GROUPS/PHYSICS/CONFNOTES/ATLAS-CONF-2011-096/fig_08.png, 2011. Accessed: 2014-03-28. Cited on page 13.
- [21] ATLAS Collaboration. Physics at a High-Luminosity LHC with ATLAS. Jul

- 1021 2013. URL <https://cds.cern.ch/record/1564937>. Cited on page
1022 15.
- 1023 [22] J. Alwall, M. Herquet, F. Maltoni, O. Mattelaer, and T. Stelzer. MadGraph
1024 5: going beyond. *Journal of High Energy Physics*, 6:128, June 2011. doi:
1025 10.1007/JHEP06(2011)128. Cited on page 15.
- 1026 [23] Torbjörn Sjöstrand, Stephen Mrenna, and Peter Skands. A brief introduc-
1027 tion to {PYTHIA} 8.1. *Computer Physics Communications*, 178(11):852 –
1028 867, 2008. ISSN 0010-4655. doi: [http://dx.doi.org/10.1016/j.cpc.2008.
1029 01.036](http://dx.doi.org/10.1016/j.cpc.2008.01.036). URL [http://www.sciencedirect.com/science/article/
1030 pii/S0010465508000441](http://www.sciencedirect.com/science/article/pii/S0010465508000441). Cited on page 15.
- 1031 [24] The ROOT Team. Root. <http://root.cern.ch/drupal/>, 2014. Ac-
1032 cessed: 2014-03-28. Cited on page 15.
- 1033 [25] S. Agostinelli, J. Allison, K. Amako, J. Apostolakis, H. Araujo, P. Arce,
1034 M. Asai, D. Axen, S. Banerjee, G. Barrand, F. Behner, L. Bellagamba,
1035 J. Boudreau, L. Broglia, A. Brunengo, H. Burkhardt, S. Chauvie, J. Chuma,
1036 R. Chytracek, G. Cooperman, G. Cosmo, P. Degtyarenko, A. Dell'Acqua,
1037 G. Depaola, D. Dietrich, R. Enami, A. Feliciello, C. Ferguson, H. Fe-
1038 sefeldt, G. Folger, F. Foppiano, A. Forti, S. Garelli, S. Giani, R. Gi-
1039 annitrapani, D. Gibin, J.J. Gómez Cadenas, I. González, G. Gracia
1040 Abril, G. Greeniaus, W. Greiner, V. Grichine, A. Grossheim, S. Guatelli,
1041 P. Gumligner, R. Hamatsu, K. Hashimoto, H. Hasui, A. Heikkinen,
1042 A. Howard, V. Ivanchenko, A. Johnson, F.W. Jones, J. Kallenbach, N. Kanaya,
1043 M. Kawabata, Y. Kawabata, M. Kawaguti, S. Kelner, P. Kent, A. Kimura,
1044 T. Kodama, R. Kokoulin, M. Kossov, H. Kurashige, E. Lamanna, T. Lampén,
1045 V. Lara, V. Lefebure, F. Lei, M. Liendl, W. Lockman, F. Longo, S. Magni,
1046 M. Maire, E. Medernach, K. Minamimoto, P. Mora de Freitas, Y. Morita,
1047 K. Murakami, M. Nagamatu, R. Nartallo, P. Nieminen, T. Nishimura, K. Oht-
1048 subo, M. Okamura, S. O'Neale, Y. Oohata, K. Paech, J. Perl, A. Pfeiffer,
1049 M.G. Pia, F. Ranjard, A. Rybin, S. Sadilov, E. Di Salvo, G. Santin, T. Sasaki,
1050 N. Savvas, Y. Sawada, S. Scherer, S. Sei, V. Sirotenko, D. Smith, N. Starkov,
1051 H. Stoecker, J. Sulkimo, M. Takahata, S. Tanaka, E. Tcherniaev, E. Safai
1052 Tehrani, M. Tropeano, P. Truscott, H. Uno, L. Urban, P. Urban, M. Verderi,
1053 A. Walkden, W. Wander, H. Weber, J.P. Wellisch, T. Wenaus, D.C. Williams,
1054 D. Wright, T. Yamada, H. Yoshida, and D. Zschiesche. Geant4—a sim-
1055 ulation toolkit. *Nuclear Instruments and Methods in Physics Research*
1056 *Section A: Accelerators, Spectrometers, Detectors and Associated Equip-
1057 ment*, 506(3):250 – 303, 2003. ISSN 0168-9002. doi: [http://dx.doi.org/
1058 10.1016/S0168-9002\(03\)01368-8](http://dx.doi.org/10.1016/S0168-9002(03)01368-8). URL <http://www.sciencedirect.com/science/article/pii/S0168900203013688>. Cited on page 17.
- 1059 [26] ATLAS Collaboration. Performance assumptions for an upgraded ATLAS
1060 detector at a High-Luminosity LHC. Mar 2013. URL [https://cds.cern.
1061 ch/record/1527529/](https://cds.cern.ch/record/1527529/). Cited on pages 17, 20, 26, 27, and 28.
- 1062 [27] ATLAS Collaboration. Electron performance measurements with the ATLAS

1064 detector using the 2010 LHC proton-proton collision data. *Eur. Phys. J. C*,
1065 72(arXiv:1110.3174. CERN-PH-EP-2011-117):1909. 45 p, Oct 2011. Com-
1066 ments: 33 pages plus author list (45 pages total), 24 figures, 12 tables, sub-
1067 mitted to Eur. Phys. J. C. Cited on pages 26 and 28.

1068 [28] ATLAS Collaboration. Search for New Phenomena in Monojet plus Missing
1069 Transverse Momentum Final States using 10fb-1 of pp Collisions at $\sqrt{s}=8$
1070 TeV with the ATLAS detector at the LHC. Nov 2012. URL [http://cds.
1071 cern.ch/record/1493486/](http://cds.cern.ch/record/1493486/). Cited on pages 32 and 33.

1072 [29] Donald Duck. The history of automatic control. *Duckburg Journal of Sci-
1073 ence*, 106(3):345–401, 2005. Cited on page 38.

1075 **Upphovsrätt**

1076 Detta dokument hålls tillgängligt på Internet — eller dess framtida ersättare —
 1077 under 25 år från publiceringsdatum under förutsättning att inga extraordinära
 1078 omständigheter uppstår.

1079 Tillgång till dokumentet innebär tillstånd för var och en att läsa, ladda ner,
 1080 skriva ut enstaka kopior för enskilt bruk och att använda det oförändrat för icke-
 1081 kommersiell forskning och för undervisning. Överföring av upphovsrätten vid
 1082 en senare tidpunkt kan inte upphäva detta tillstånd. All annan användning av
 1083 dokumentet kräver upphovsmannens medgivande. För att garantera äktheten,
 1084 säkerheten och tillgängligheten finns det lösningar av teknisk och administrativ
 1085 art.

1086 Upphovsmannens ideella rätt innehåller rätt att bli nämnd som upphovsman
 1087 i den omfattning som god sed kräver vid användning av dokumentet på ovan
 1088 beskrivna sätt samt skydd mot att dokumentet ändras eller presenteras i sådan
 1089 form eller i sådant sammanhang som är kränkande för upphovsmannens litterära
 1090 eller konstnärliga anseende eller egenart.

1091 För ytterligare information om Linköping University Electronic Press se för-
 1092 lagets hemsida <http://www.ep.liu.se/>

1093 **Copyright**

1094 The publishers will keep this document online on the Internet — or its possi-
 1095 ble replacement — for a period of 25 years from the date of publication barring
 1096 exceptional circumstances.

1097 The online availability of the document implies a permanent permission for
 1098 anyone to read, to download, to print out single copies for his/her own use and
 1099 to use it unchanged for any non-commercial research and educational purpose.
 1100 Subsequent transfers of copyright cannot revoke this permission. All other uses
 1101 of the document are conditional on the consent of the copyright owner. The
 1102 publisher has taken technical and administrative measures to assure authenticity,
 1103 security and accessibility.

1104 According to intellectual property law the author has the right to be men-
 1105 tioned when his/her work is accessed as described above and to be protected
 1106 against infringement.

1107 For additional information about the Linköping University Electronic Press
 1108 and its procedures for publication and for assurance of document integrity, please
 1109 refer to its www home page: <http://www.ep.liu.se/>